SSRG International Journal of Civil Engineering
ISSN: 2348-8352/ https://doi.org/10.14445/23488352/IJCE-V13I8P110

Volume 13 Issue 8, 172-182, August 2026

Original Article

Effect of Instability Factors under Compressive Loads for Metal Structures: Residual Stresses and Geometric Imperfections

Manuela Yannela Huaman Melgarejo[1], Luis Fernando Upiachihuay Rosales[1], Marx Anthony Chahuayo Fernandez[1], Giancarlo Fernando Meza Terbullino[1*]

[1]*School of Civil Engineering, Universidad Continental, Huancayo, Junín, Perú.*

[*]*Corresponding Author : gmezat@continental.edu.pe*

Received: 26 April 2026 Revised: 25 June 2026 Accepted: 24 July 2026 Published: 31 August 2026

Abstract *- The consideration of geometric imperfections and residual stresses are inevitable in the compression design of metallic structures that are prone to buckle; nonetheless, the sensibility of these parameters to compression stresses lead to their collapse that trigger the loss of human lives and to the cost increase of the construction sector without a previous analysis. Thus, the evaluation of the influence of geometric imperfections in residual stresses in elements subjected to compressions tresses for different degrees of slenderness was proposed. With the aim to attain this, a procedure focused on the stated frameworks of the American Institute of Steel Construction (AISC), the Building Technical Code SE-A (CTE) and the sensitivity analysis for the critical load in the Finite Element model. The results showed that the AISC values for torsional and flexural buckling are often higher than the CTE guide. Also, for thin objects, the effect of imperfections in shape and remaining stresses can make the material weaker. Finally, it has been decided that these instability effects need to be considered in slender elements according to the CTE guide. This means that the reduced slenderness (λ0) should be taken into account if the AISC code is used to evaluate buckling loads.*

Keywords *- Buckling, Critical load, Instability, Rolled profile.*

1. Introduction

Nowadays, reinforced concrete and structural Steel are the most employed materials in the construction sector, within the buildings, the vertical elements (during their service life) tend to be in constantly under compression stresses, which makes them an element prone to instability (also known as buckling) [1]. The configuration of this effect is independent from the compression resistance, but dependent on the dimensional features of the element during the elastic lineal stage until the geometric nonlinearity [2]. Metal profiles with thin and often open cross-sections can be unstable because of local and distortional buckling. This is mainly caused by geometric imperfections and residual stresses, which affect how much the material can bear loads. This is a common practice in civil engineering, as using software to fully assess stability loss can sometimes lead to solutions that are not optimal or pose risks [3, 4].

The elements of the Steel are manufactured industrially for each typology. Nevertheless, the manufacturing process are generally welded or rolled [5]. The manufacturing process of the welded elements come from the joining of sections that were rolled through automatic or electric arc processes. Whereas, the rolled profiles are manufactured through hot or cold rolling (mechanical transformation) [6]. To choose either of the manufacturing methods generates, in the elements itself, geometric imperfections and residual stresses inevitably.

Geometric imperfections are small deviations that are generated in the elements, these are not visibly perceivable, but have influence in a greater deformation. This mechanism is translated to small geometric curves of the element in respect to totally straight dimensions [7]; likewise, residual tensions is another phenomenon that is produced in the material due to the disproportionate cooling process after the manufacturing phase. The internal part of the element has a different cooling degree when compared to the external part. These effects were studied in different experimental researches that compare the presence of different tensile stresses accumulated in each concrete zone of the Steel structural element [8]. Besides, it was identified that these stress magnitudes that are generated within the element are caused mainly by the geometric dimensions and the cooling level [9]. Current standards, like the American Institute of Steel Construction (AISC) for Steel structures [10] and the Construction Technical Code (Structural Safety SE-A) [11] consider values of "χ" for different buckling curves that avoid these types of phenomena. However, in some cases, it is necessary to determine the influence, particularly separately, with the objective of the analysis to be more reliable [12].

The alternative to determine the self-value that derives from the buckling reduction is to do the analysis of deflections called second-order analysis or non-linear geometric analysis UNE EN 1993-1-1 [13]. Additionally, the critical load has to be considered as the starting point of the analysis [14, 15], the factors associated to the geometric imperfection and residual stresses is later implemented, which tend to significantly represented in the behavior of the element. Another approximation method in these cases is the employment of the Finite Element approach that can also be used with the purpose to guarantee the structural behavior [15].

The investigation performed by Irvin [16], proposes to perform the calculations of local buckling of welded-type slender columns under buckling curves stipulated on the Annex B in the EN 1993-1-5 [17], as a verification of the resistance for the geometric imperfection design, and the residual stresses that have to be adequately selected.

Some studies have looked at H-type metal profiles to see how much pressure and how well-made they are. But these studies suggest [18, 19] that they could be used for other types of profiles in the same family, and that they could be used for reduced slenderness ($\lambda 0$) in a wider way. In this case, IPE-type profiles are one of the most marketed products in different countries.

The research studied by [4] looked at how strong and stable steel columns are when they are filled with concrete. It found that open sections of metal profiles are more likely to become unstable in different ways than short columns. This mainly affects local and distortional buckling. Another study looked at how different types of imperfections affected the behaviour of metal profiles. It found that if the initial geometry was imperfect, the amplitude of instability increased. This led to an increase in the critical load value, and the metal profile became unstable.

Nonetheless, the experimental approaches also have a better approximation when applying rotational elastic restrictions for examining the buckling from a slenderness ratio, obtaining a probabilistic analysis with approximately 95% of confidence, which makes this model contribute as a predictive simulation [20].

The aim of this research is to separately evaluate the influence of residual stresses and geometric imperfections in IPE-type steel profiles (thin web). This is mainly within the regulatory framework of the CTE and a practical verification through the AISC. This is because it provides a parametric sensitivity analysis that maps the nonlinear interaction between both factors. The aim is to identify their contribution to the reduction of load-bearing capacity.

2. Materials and Methods

In this research, the buckling behavior under compression loads in a steel profile of the type IPE 240 is firstly considered, this means that the design is not very strong and thin for the lengths given in the table.
1. For this, different degrees of slenderness (λ) are considered. In first place, verification of the effect of the critical load through the Euler's theorem and the numerical method, in this verification process, the lineal elastic effect and the non-lineal geometry were considered, while also employing structural analysis approaches, [21] critical loads and buckling modes [22].

2.1. Analysis Model

The metal profiles are generally employed because they cover large distances within a structure, they also offer design versatility, mechanical resistance, and assembly transportation efficiency [23]. With the objective to understand the buckling behavior of these elements, a vertical element with a restricted support in its axis and another one with lateral displacement restriction were analyzed, as exhibited in Figure 1., this idealization correspond to design cases usage category for industrial buildings, warehouses, and agricultural and rural houses [24].

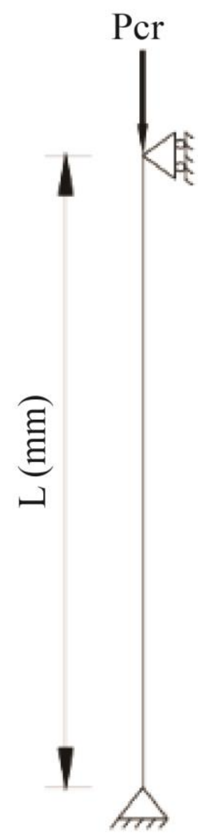

Fig. 1 Example for small figure

Table 1. Slenderness for each defined height

Type	iy (mm)	iz (mm)	Length (mm)	K factor (articulated - articulated)	Slenderness λ
IPE 240	99.7	26.9	1400	1	50
IPE 240	99.7	26.9	1900	1	70
IPE 240	99.7	26.9	2400	1	90
IPE 240	99.7	26.9	2950	1	110
IPE 240	99.7	26.9	3500	1	130
IPE 240	99.7	26.9	4050	1	150
IPE 240	99.7	26.9	4550	1	170
IPE 240	99.7	26.9	5000	1	185

The selected metal profile, with the objective to evaluate its behavior under compressions, was stablished according to different heights in order to stablish the slenderness category, which are depicted on Table 1.

2.1.1. Lineal Analysis

The lineal solutions of a structure is governed by a matrix Equation that related the equilibrium among the generalized stresses. $\boldsymbol{f^g}$ with the generalized displacements $\boldsymbol{d^g}$ through the assembly of the stiffness of each element $\boldsymbol{k^g}$.

$$f^g = k^g * d^g \qquad (1)$$

The procedure of this analysis is constituted from the reprocess (a structure that ranges from the assembly of the stiffness matrix of each element and the connectivity that exists among them). Another reprocess (actions centered in the existence of actions that are applied in each node of the element). And the convergence is done by imposing kinematic boundary conditions that simplify the solution for obtaining the displacements and rotations in the structure [25].

By employing the beam theory, the stiffness Timoshenko matrix for plain problems of 6 x 6 elements was used [18], considering the 6 degrees of freedom that are distributed 3 in each node of the beam and the shear factor on Equation 2, unlike the Navier Bernoulli theorem that assumes shear in deformability $\boldsymbol{\alpha \to 0}$.

$$\alpha = \frac{12EI_z}{GA_{Vy}L^2} \qquad (2)$$

Where: "E" is the elasticity module of the material, "I_z" is moment of inertia around the z axis, "G" is the shear module that depends on the Poisson coefficient, "A_{Vy}" is the shear area of the section, and "L" is the length of the material.

2.1.2. Geometric Non-Lineal Analysis

The second-order theory araised based on the hypothesis that small displacements in the lineal theory do not provide precise results. Nevertheless, this non lineal behavior is linked to big displacements that depend on the geometry of the element (Length), like the P-Delta effect, where through P action load, the structure experiments a horizontal displacement [26].

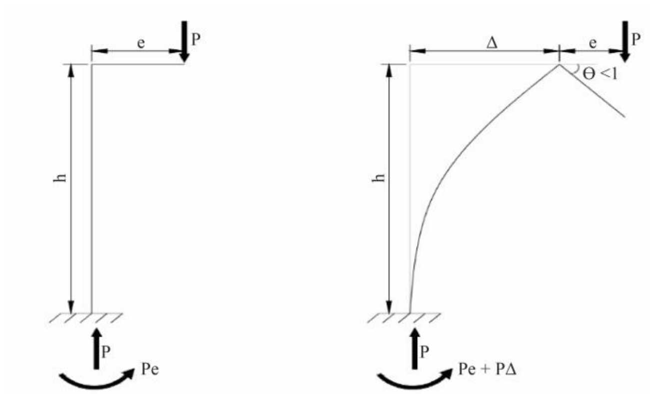

Fig. 2 P-Delta effect on a structure

A good approximation of the non-lineal stiffness comprises the sum of the matrix with a lineal stiffness. $\boldsymbol{k^{lin}}$ Plus, the geometric stiffness matrix $\boldsymbol{k^{geo}}$, which assumes a precise approximation for values of the axial stress with a margin of 25% in relation to the critical axial stress of the structure [27]. Considering that analysis, a significant Equation of the non-lineal behavior involves the assembly of the global matrix based on the non-lineal stiffness matrix of the element, as exposed on Equation (2).

$$f' = [\![(k]\!]^{lin} + k^{geo}[N^e{}_x\,]) * d' \qquad (2)$$

Where: "$\boldsymbol{f'}$" is the load vector, "$\boldsymbol{k^{lin}}$" is the linear stiffness matrix, "$\boldsymbol{k^{geo}}$" is the geometric stiffness matrix that depends on "$\boldsymbol{N^e{}_x}$", "$\boldsymbol{N^e{}_x}$" is the group of values of axial stress for each element, and "$\boldsymbol{d'}$" is the vector that groups the freedom degrees no are not constrained.

Subsequently, the non-lineal behavior involves a group of steps that require the already defined elastic analysis and considering the geometry of the element, a series of iterative steps is determined, as indicated below.

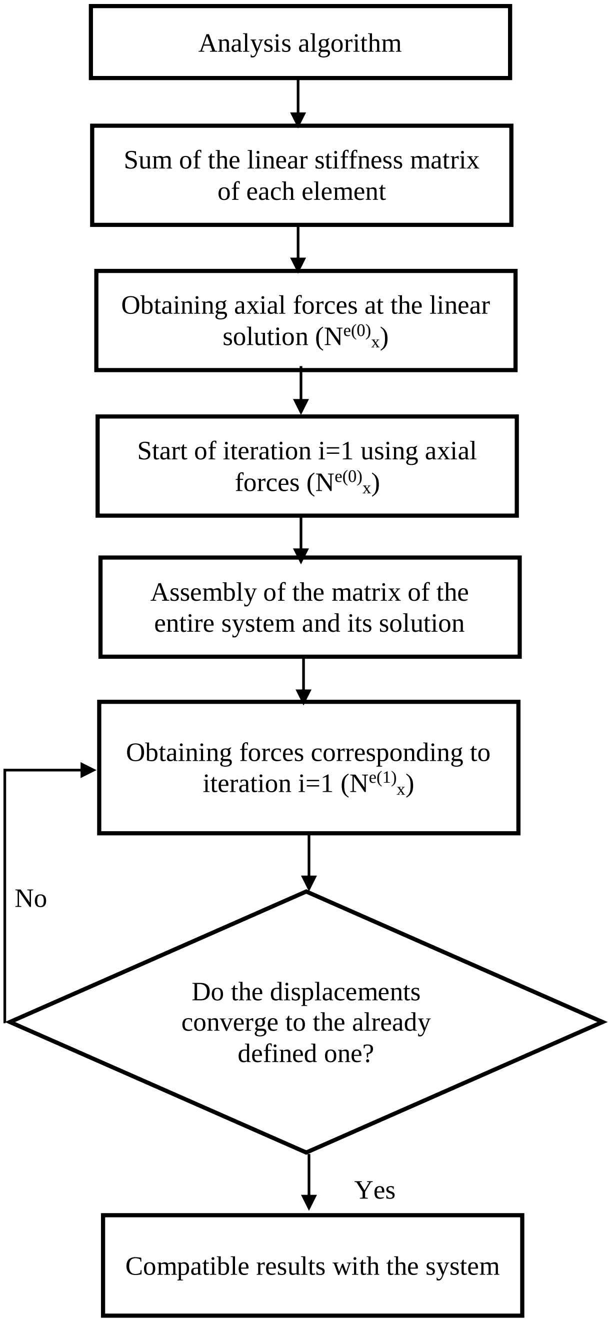

Fig. 3 Flowchart of geometric non-linear analysis

2.2. Instability

2.2.1. Numeric Approach

If we add proportionally the load P and the load Factor F, as shown in Figure 5, considering an element with a stiffness k and a displacement u, these are governed by a factor λ that increases gradually with the aim to the dynamic incidences not to be significant, and under the vertical equilibrium of the system that contains an axial stress equal to P, there is an equivalent equation for the horizontal stresses (see Equation 3).

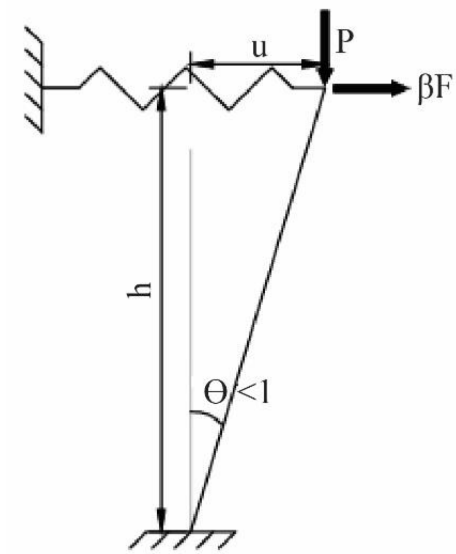

Fig. 4 Equilibrium of the geometric system

$$\boldsymbol{\beta F} = (\boldsymbol{K} - \boldsymbol{\beta}\ \boldsymbol{P}/\boldsymbol{L}) * \boldsymbol{u} \qquad (3)$$

When the value $\beta \geq \beta_{crit}$ the balance within the system turns to be indifferent, and the value of u can take negative or positive values from the transition point. Besides that, once the critical factor is surpassed, the structure turns unstable, as exhibited in Figure 6.

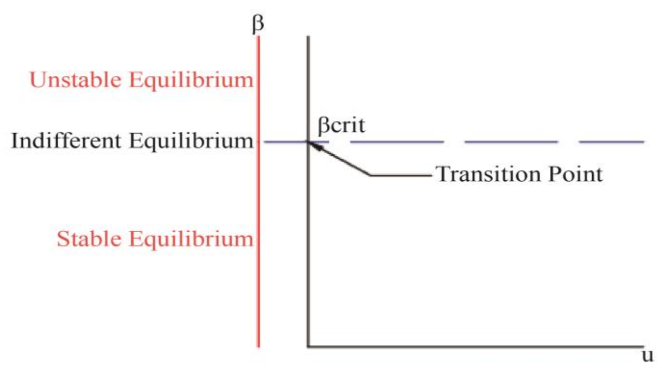

Fig. 5 Instability of the system

Hence, an approximate manner to calculate the critical factor (β_{crit}) that connects the previously mentioned conditions through the adjacent equilibrium analysis satisfied the following condition.

$$\det\left(k^{lin} + k^{geo}[N^e{}_x(\beta)]\right) = 0 \qquad (4)$$

Nevertheless, it should be considered that in order to obtain the most approximate results of the critical load, the total length has to be discretized, this means that the small that conform the length have to be considered until reducing the error, as depicted on Figure 1.

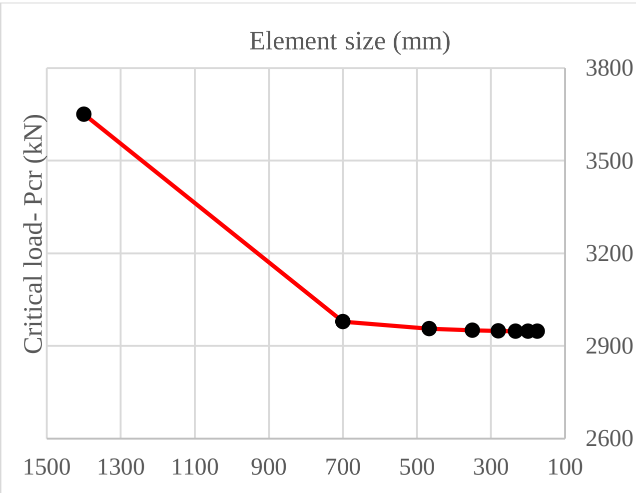

Fig. 6 Tlement size for the λ-50 model

2.2.2. Euler's Theorem

Euler's theorem is focused on the study of a straight element subjected to compressive stresses under boundary condition constraints (supports and hinges). The critical load nomenclature is associated when the element is placed in a transition point that goes from a stable equilibrium to an unstable state or to an indifferent equilibrium. Thus, the first critical load is denominated as Euler's formula, and it is determined as follows:

$$P_{cr,1} = \frac{EI_z}{{L_e}^2} \tag{5}$$

Where: "$P_{cr,1}$" is the critical load of the first mode, "I_z" is the moment of inertia around the z axis e, "E" is the elasticity module of the, "L_e" is the equivalent length that depends on the length of the element and the boundary condition factor.

To make sure the finite element model (FEM) was accurate, a mesh convergence study was carried out. This involved splitting the element length into smaller parts. This is done to make sure the numbers are completely stable, because making the mesh finer doesn't really matter. This makes the calculations cheaper and gets rid of any random modelling assumptions.

2.3. Residual Stresses

These are the internal stresses that make fibres break and cause a loss of bendiness long before the theoretical ideal load is reached. To study this effect on its own in the numerical model, a practical approach based on reducing the effective yield limit [25, 28] described in Equation 6, was used.

In hot-rolled sections, this limit is usually set between 30% and 50% of the material's lost strength [29]. However, in this study, for a broader scope, it was considered between 10% and 50% $f_{y;R}$.

$$\chi^{TR} = (1 - f_{y;R}) + f_{y;R}.\left[1 - \left(\frac{\lambda_0}{\lambda_{lim}}\right)\right] \tag{6}$$

Where: "$f_{y;R}$" is the maximum percentage of residual stress, "λ_{lim}" is the smallest reduced slenderness that can be achieved, "χ^{TR}" is a value representing the reduction factor due to residual stresses, and "λ_0" is the reduced slenderness.

2.4. Geometric Imperfection

Geometric imperfection is when something is not perfectly vertical. These can be shown as an inclination angle (θ_1) using Equation 7, where it is modelled as an equivalent horizontal force (see Figure 7).

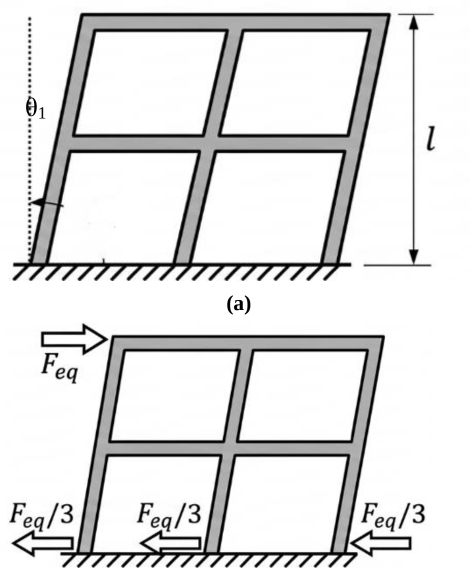

Fig. 7 This is how we represent the geometric imperfection: (a) The angle of slope, (b) How the force is the same but in a different way.

$$\theta_1 = \theta_0\, \alpha_h\, \alpha_m \tag{7}$$

$$\alpha_h = 2/\sqrt{l} \;\; , 2/3 \le \alpha_h \le 1$$

$$\alpha_m = \sqrt{0.5(1 + 1/m)}$$

Where: "θ_0" is the basic value, "2/3 ≤ α_h ≤ 1" is the reduction coefficient for length or height, and "α_m" is the reduction coefficient for the number of elements.

2.5. Geometric Imperfections and Residual Stresses are Linked

The Technical Building Code for checking flexural buckling limits the minimum buckling value between the two less resistant directions of the section and the torsion of the steel profile. The procedure that determines the nominal strength $N_{b,Rd}$ uses buckling curves to estimate the imperfection coefficient (α), the reduced slenderness of the profile (λ_0), and the reduction factor (χ) as a function of $\emptyset$, as shown in Equation 8.

$$N_{b,Rd} = \chi . f_y . A \quad (8)$$

$$\chi = \frac{1}{\emptyset + \sqrt{\emptyset^2 - \bar{\lambda}^2}}$$

$$\emptyset = 0.5\left[1 + \alpha\left(\bar{\lambda} - 0.2\right) + {\lambda_0}^2\right]$$

Where: The letter "A" is the area of the profile. The letter "f_y" is the yield strength of the profile. The letter "γ_{M0}" is the partial safety factor. Also, for the "α" factor, the geometric imperfection and residual stresses are already included.

The AISC guide, on the other hand, provides easier methods for calculating the reduction factor (χ) when working out the upper and lower values of the reduced slenderness (λ0) [10], as shown in Equation 9.

$$\lambda_0 \leq 1.5 \qquad \chi \leq 0.658^{{\lambda_0}^2} \quad (9)$$

$$\lambda_0 > 1.5 \qquad \chi \leq \frac{0.877}{{\lambda_0}^2}$$

3. Results

3.1. Flexural and Torsional Buckling (AISC – CTE)

Figures 8 and 9 show how the metal profile's flexibility and resistance to twisting are tested. These calculations are based on the typical way that considers geometric imperfections and residual stresses. As you can see in Figure 8, when the element is slenderer (λ = 170), the nominal strength is almost completely reduced because of the flexural buckling that develops in the weak axis.

We can see that the AISC technical guide estimates the nominal strength to be around 16% higher than the CTE guide for 70 ≤ λ ≤ 130, when considering the reduction coefficients of curve c. Using the same approach to compare torsion, as shown in Figure 9, we see that for 70 ≤ λ, there is a variation of around 11%. The changes are due to the practical applications defined by each guide. These are based on the reduction factor (χ), which is the result of instability (geometric imperfection and residual stresses). However, the decoupled analysis of these variables is defined in the following sections.

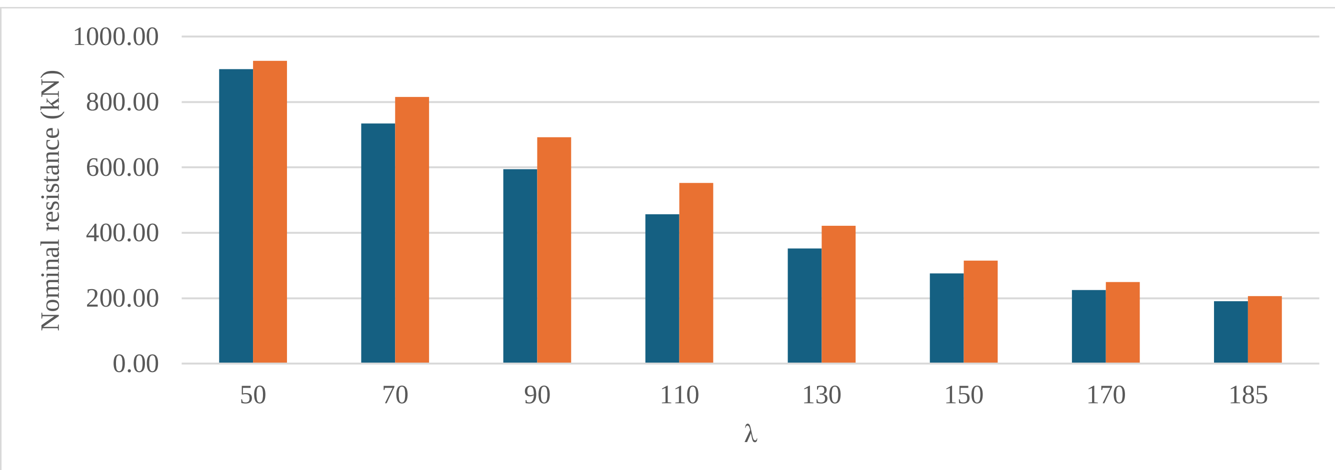

Fig. 8 Flexural and torsional buckling for different slenderness levels

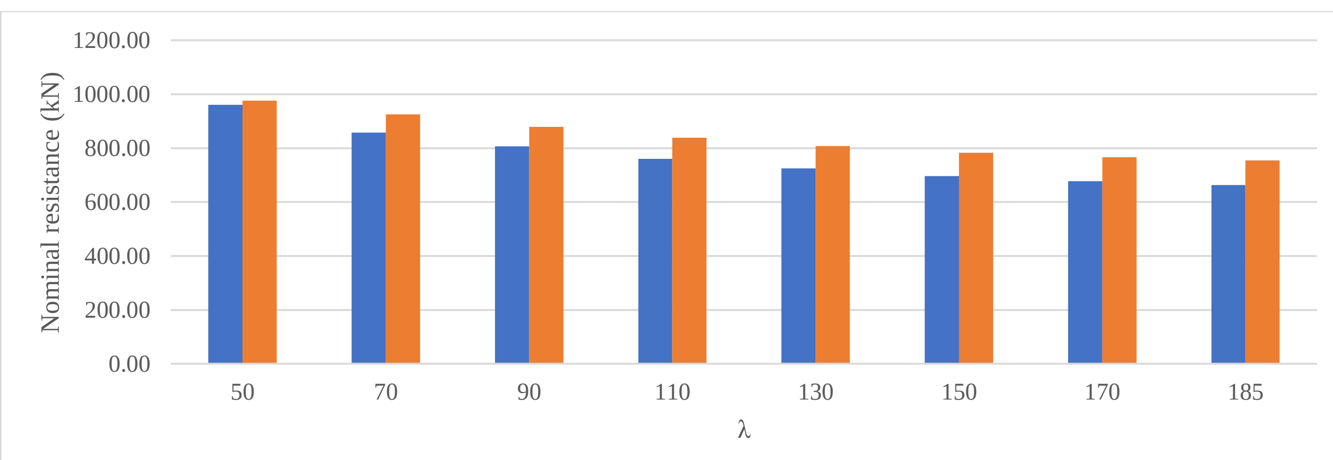

Fig. 9 Torsional buckling for different slenderness levels

3.2. Critical Buckling Load without Instability Effects

In Figure 10, the first buckle mode is illustrated, discretizing 4 elements that represent sizes of 460 mm for the model λ-50. Following this procedure, it was applied the other slenderness models and later it was compared to Euler's theorem, which are shown in Table 2. You can notice that as the element becomes less slender, the Euler model becomes slightly less accurate compared to the numerical model.

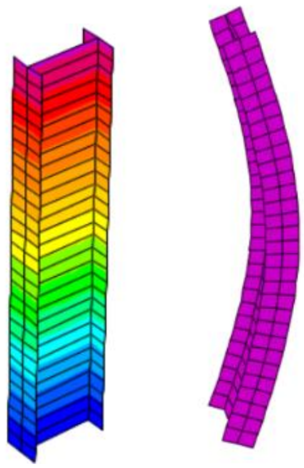

Fig. 10 Shape of the first buckling mode

Table 2. Instability of the system

λ	Euler (Pcr)	Numerical (Pcr)	%
50	3003.18	2948.05	1.87%
70	1630.54	1614.16	1.01%
90	1021.92	1015.48	0.63%
110	676.38	673.56	0.42%
130	480.51	479.09	0.30%
150	358.86	358.07	0.22%
170	284.32	283.83	0.17%
185	235.45	235.11	0.14%

3.3. Instability Effects

In figure 11, the effect that produces geometric imperfection in each slenderness of the element is exhibited, the effect of this phenomenon makes the element to fail because if the instability before reaching the critical buckling load for each model as established in Table 2; also, when is the element is more slender (λ=185) it has to admit very small axial loads (P = 117 kN) in comparison to elements that are less slender (λ=50) that admit higher loads (P = 1481 kN). In addition, in spite of the fact that these elements tolerate more deformation, the critical load is reduced even more, that it becomes much more sensitive.

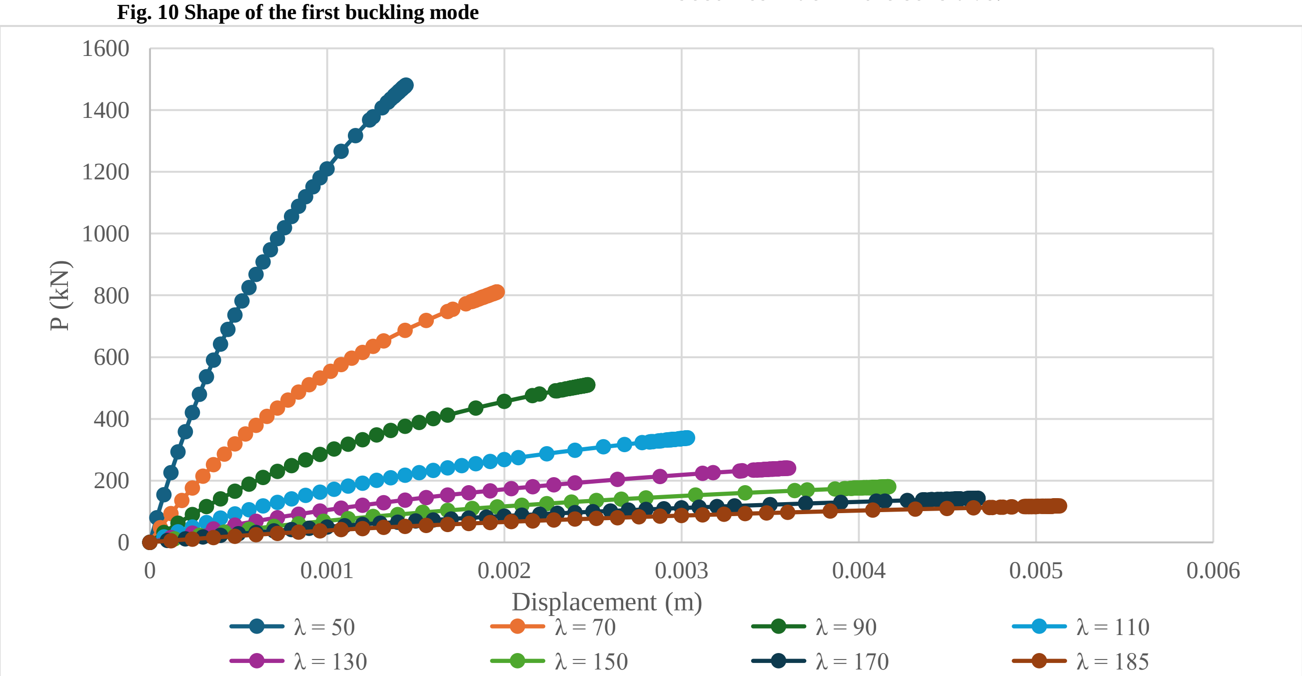

Fig. 11 Load-displacement relationship for each model

Figure 12 shows the reduction coefficients for each reduced slenderness ratio considering only residual stresses, as established by the normative considerations: TR+IG (AISC) and TR+IG (CTE) for calculating the reduction factor (χ) already account for the effects of geometric imperfections and residual stresses. Furthermore, for the models (TR = 10% - 50%), the reduction factors decrease as the slenderness ratio decreases. However, starting from a reduced average slenderness ratio (λ0 = 1.3), they no longer depend on the variation of residual stresses. On the other hand, the choice of reduction coefficients will depend on the methodology used, as seen in the λ-50 (AISC) and λ-50 (CTE) factors. The curve showing the 30% residual stress is similar to the other curves (10% or 50%).

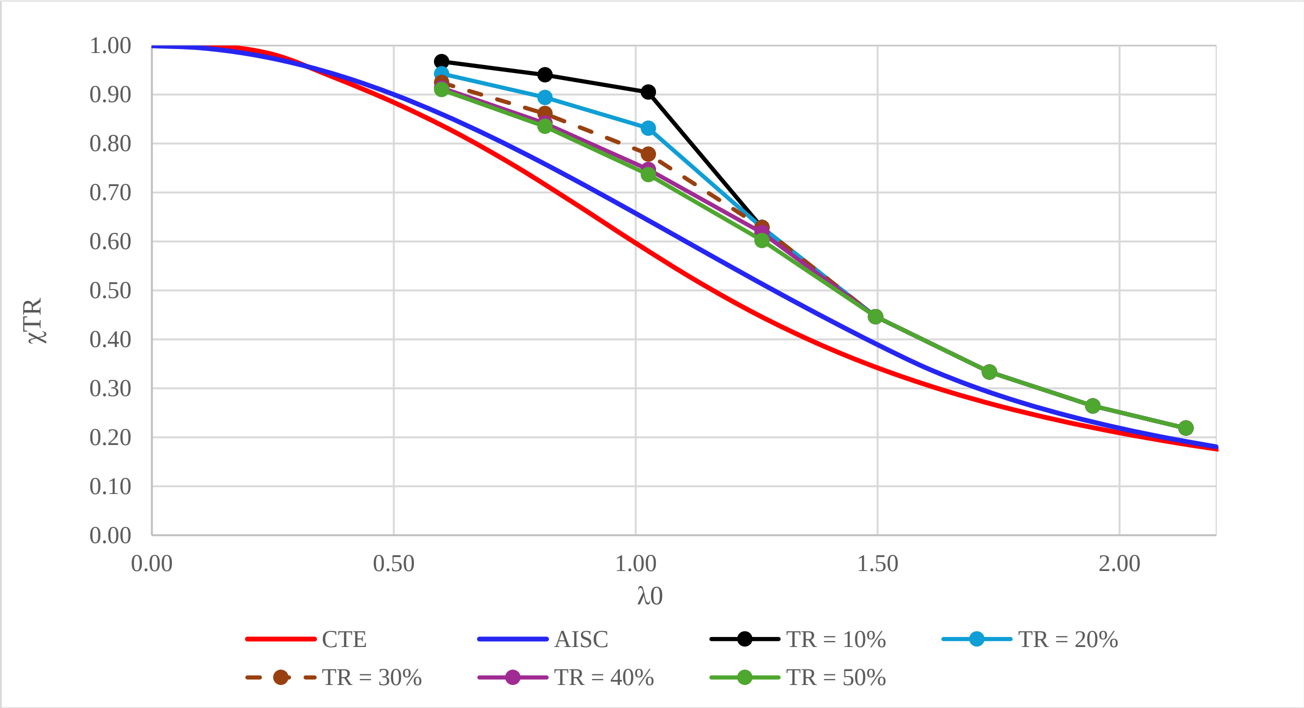

Fig. 12 Effect of residual stresses on the reduction coefficients

3.4. Coupled Geometric Imperfection and Residual Stresses

Figure 13 shows the reduction coefficients for each reduced slenderness ratio. These take into account both residual stresses and geometric imperfections. The AISC and CTE design guides both use curves that approximate the IPE 240 model with 30% RS. However, when we use more slender elements, they tend to be similar.

The CTE guide is stricter than the AISC guide when it comes to these unstable effects on the reduction coefficients of rolled profiles. This is because for curves b, c, and d, approximately $\lambda 0 < 2.25$. We can also see that the IPE model overestimates compared to curve c in the range around $1.0 < \lambda 0 < 2.0$. And around $\lambda 0 < 1.26$, the AISC guide overestimates.

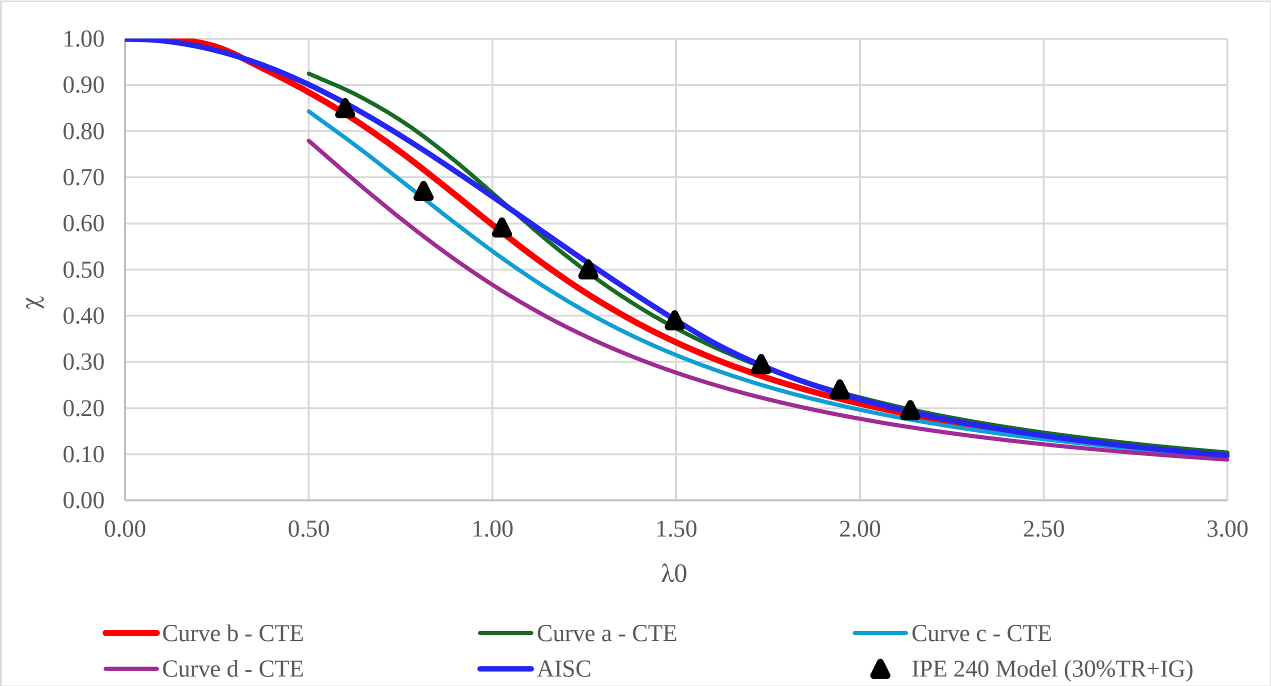

Fig. 13 Effect of residual stresses on the reduction coefficients

4. Discussion

Practising with numbers or analysing data helps you understand how a model shows nonlinear effects related to instability [13]. This brings an idea of how the resistance capacity of the materials is reduced due to the effects of the residual stresses and the geometric imperfections, leaving significance in the coefficients of reduction because of not considering these effects [30].

The metallic profiles can suffer different tensile demands that, in this case, usually have higher sensitivity under compressions stresses [31], in which the AISC and CDT guidelines contemplate these effects in the buckling and torsional verifications; however, the CTE considers the torsional buckling as a conventional verification that is restrictive. This measure is meaningful in less slender elements, as it is detailed in Figure 8.

The geometric imperfection triggers an additional stress in the element that involves to tolerate a critical load that is much lower that the Euler's buckling [32], and this, at the same time, makes it much more sensible to very slender elements, although they develop higher deformation [30].

The residual stress is one of the incident factors in the resistance capacity of metal structures [33], which is appropriate when the manufacturing process generates uncertainty, as a consequence, ranges of residual stresses are stablished (10% - 50%) that are reflected in the reduction coefficient (χ^{TR}). However, when the reduced slenderness (λ_0) is higher than 1.3, it no longer depends on the variation of the residual stresses. This occurs because the material fails in the elastic stage and does not achieve the plastification in any of the section.

Finally, when determining the reduction factor (χ) for the verification of the metallic structures, the guidelines provide a scope for conventional structures [30, 34], nonetheless, for singular cases like very slender elements and a high rate of manufacturing errors, these considerably affect in the geometric imperfection and the residual stresses by reducing, each time, this reduction factor as exhibited in figure 11. On the other side, the standards employ different curves for this coefficient (χ), but the methodology entails a similar analysis because both contemplate these instability effects with the purpose to avoid the over-dimensioning in metal structures. Additionally, acceptable values for the elastic calculation mean to stay away from the critical load by 10% [33]. However, the CTE's C curve, which considers these unstable effects, is better to use when $1.0 < \lambda 0$. For all the other cases, the B curve can be used, as these ranges were confirmed in experiments and computer simulations by [19].

One way to deal with these unstable effects that alter the critical load is to fill them with concrete. This significantly improves deformation and can even double the load capacity, especially for this family of metal profiles [4].

5. Conclusion

One of the most important requisites for designing a metallic structure is the instability behavior, where they get affected by two important factors, which are: geometric imperfection, and the residual stresses for different degrees of slenderness.

It has been verified that through the Finite Element model, the geometric imperfection causes a reduction in the tolerance of the actions, which make it more susceptible in elements with a higher slenderness. Besides this, the residual stresses are added to these effects, depending on this variation (10% - 50%) up to $\lambda_0 < 1.3$ and after this, the variation of the residual stresses are not relevant anymore.

As the main idea in the verification of the buckling in rolled metallic profiles, the regulatory standards as the American Institute of Steel Construction and the Technical Edification Code SE-A, stablish that these already included instability effects for determining the reduction factor. However, when the element is too slender and had a high rate of uncertainty in the manufacturing error, then a higher relevance in these instability errors should be taken into account. If $\lambda 0$ is less than 1.0, it is better to use the CTE curves.

It is recommended, in future researches, for these vertical elements subjected to compressive actions, to propose structural configurations that help to maintain the resistance capacity against these instability effects.

Acknowledgements

Thanks to all the collaborators of this research with their knowledge and contribution to structural engineering; likewise, thanks to the scientific journal for providing the author's guidelines.

References

[1] Juan Carlos Pomare et al., "Safety Issues in Buckling of Steel Structures by Improving Accuracy of Historical Methods," *International Journal of Environmental Research and Public Health*, vol. 18, no. 22, pp. 1-21, 2021. [CrossRef] [Google Scholar] [Publisher Link]

[2] WFEO Disaster Risk Management Committee, *Engineering and Resilience in Disaster Risk Management for Sustainable*, pp. 1-37, 2022. [Publisher Link]

[3] Katarzyna Rzeszut, "Post-Buckling Behaviour of Steel Structures with Different Types of Imperfections," *Applied Sciences*, vol. 12, no. 18, pp. 1-21, 2022. [CrossRef] [Google Scholar] [Publisher Link]

[4] Nadia Gouide et al., "Axial Behavior and Stability of Built-Up Cold-Formed Steel Columns with and without Concrete Infill: Experimental and Numerical Investigation," *Computer Modeling in Engineering & Sciences*, vol. 145, no. 1, pp. 457-481, 2025. [CrossRef] [Google Scholar] [Publisher Link]

[5] Manmohan Dass Goel et al., "An Abridged Review of Buckling Analysis of Compression Members in Construction," *Buildings*, vol. 11, no. 5, pp. 1-17, 2021. [CrossRef] [Google Scholar] [Publisher Link]

[6] Jifeng Xu, Qun Zhao, and Pizhong Qiao, "A Critical Review on Buckling and PostBuckling Analysis of Composite Structures," *Frontiers in Aerospace Engineering*, vol. 2, no. 3, pp. 157-168, 2013. [Google Scholar]

[7] Yong-Lin Pi, and N. S. Trahair, "In-Plane Buckling and Design of Steel Arches," *Journal of Structural Engineering*, vol. 125, no. 11, pp. 1291-1298, 1999. [CrossRef] [Google Scholar] [Publisher Link]

[8] Jonas Nonn, Vera Wilden, and Markus Feldmann, "A Consistent Approach for Global Buckling of Steel Structures," *Steel Construction Steel Construction*, vol. 16, no. 2, pp. 93-104, 2023. [CrossRef] [Google Scholar] [Publisher Link]

[9] Ben Young, "Local Buckling and Shift of Effective Centroid of Cold-Formed Steel Columns," *Steel and Composite Structures*, vol. 5, no. 2, pp. 235-246, 2005. [Google Scholar]

[10] Jack McCormac, and Stephen Csernak, *Maple Construction Design*, Alfaomega, 2013. [Google Scholar]

[11] Technical Building Code (CTE), [Online]. Available: https://www.boe.es/biblioteca_juridica/codigos/codigo.php?id=424&modo=2&nota=0&tab=2

[12] K. Swaminathan et al., "Stress, Vibration and Buckling Analyses of FGM Plates—A State-of-the-Art Review," *Composite Structures*, vol. 120, pp. 10-31, 2015. [CrossRef] [Google Scholar] [Publisher Link]

[13] UNE-EN 1993-1-1:2013/A1:2014, UNE. [Online]. Available: https://www.une.org/encuentra-tu-norma/busca-tu-norma/norma?c=N0053185

[14] Marius Botis, Lajos Imre, and Mircea Conțiu, "Numerical Method of Increasing the Critical Buckling Load for Straight Beam-Type Elements with Variable Cross-Sections," *Applied Sciences*, vol. 13, no. 3, pp. 1-42, 2023. [CrossRef] [Google Scholar] [Publisher Link]

[15] Mehmed Čaušević, and Mladen Bulić, "Steel Plate Elements Subjected to Load in their Own Plane – Buckling Factors and Critical Loads," *Građevinar*, vol. 64, no. 2, pp. 115-125, 2012. [CrossRef] [Google Scholar] [Publisher Link]

[16] Irvin Quillupangui, Balázs Somodi, and Balázs Kövesdi, "Overview of FEM-Based Resistance Models for Local Buckling of Welded Steel Box Section Columns," *Applied Sciences*, vol. 14, no. 5, pp. 1-26, 2025. [CrossRef] [Google Scholar] [Publisher Link]

[17] UNE-EN 1993-1-5:2013, UNI. [Online]. Available: https://www.une.org/encuentra-tu-norma/busca-tu-norma/norma?c=N0051041

[18] J.L. Romero et al., "Finite Elements with Equivalent Distributed Actions of Any Order. Application to Timoshenko and Bernoulli-Euler Beam Models," *Construction Reports*, vol. 66, no. 535, pp. 1-18, 2014. [CrossRef] [Google Scholar] [Publisher Link]

[19] Yong Feng et al., "Axial Compression Behaviour of Welded High-Strength H-Columns Experimental Tests and Numerical Simulations," *Case Studies in Construction Materials*, vol. 19, pp. 1-16, 2023. [CrossRef] [Google Scholar] [Publisher Link]

[20] H. Yılmaz, "Buckling of Steel Plates Under Rotational Restraints: An Integration of Experimental Testing and the Vibration Correlation Technique," *Experimental Mechanics*, vol. 65, no. 6, pp. 869-884, 2025. [CrossRef] [Google Scholar] [Publisher Link]

[21] José Cegoñino, and Amaya Pérez del Palomar, *Structural Analysis. Problems*, University of Zaragoza Press, pp. 1-22, 2018. [Google Scholar] [Publisher Link]

[22] Sabina De Lis, and José Claudio, *Nonlinear Analysis Introductory Course. Applications*, University of La Laguna, pp. 1-248, 2005. [Google Scholar] [Publisher Link]

[23] Gutiérrez Aguilera, and Pedro Alexander, *Publication: Characteristics of Steel as a Structural Material*, Cooperative University of Colombia, pp. 1-13, 2023. [CrossRef] [Google Scholar] [Publisher Link]

[24] Latin American Iron and Steel Institute, *Alacero: Steel Framing: Arquitectura*, ILAFA, pp. 1-117, 2006. [Google Scholar] [Publisher Link]

[25] F. B. Varona Moya, and L. García Andión, "Linear Analysis with Limited Redistribution and the Ductility Criteria of the Sections," *Concrete and Steel*, vol. 61, no. 257, pp. 1-11, 2010. [Google Scholar] [Publisher Link]

[26] W.T. Matias Silva, A.A. Cunha, and M.P. Duque Gutiérrez, "Nonlinear Analysis of Plane Frames using the Corotational Formulation with Timoshenko Beam Element," *International Journal of Numerical Methods for Engineering Calculation and Design*, vol. 33, no. 1-2, pp. 115-122, 2017. [CrossRef] [Google Scholar] [Publisher Link]

[27] María Villoldo Lozano, "*Linear and Nonlinear Buckling of Beam Structures*," University of Madrid, pp. 1-162, 2021. [Google Scholar] [Publisher Link]

[28] Ronald D. Ziemian, *Guide to Stability Design Criteria for Metal Structures*, Wiley, pp. 1-1120, 2010. [Google Scholar] [Publisher Link]

[29] Theodore V. Galambos, and Robert L. Ketter, "Columns Under Combined Bending and Thrust," *Journal of the Engineering Mechanics Division*, vol. 85, no. 2, 1959. [CrossRef] [Google Scholar] [Publisher Link]

[30] Mariana Mohana Rodrigues da Silva, Evandro Parente Junior, and Marcelo Silva Medeiros Junior, "Study of the Influence of Geometric Imperfections and Residual Stresses on the Stability of Steel Columns Subjected to Axial Compression," *Proceedings of the 2024: XLV Ibero-Latin American Congress on Computational Methods in Engineering*, Maceco, Alagoas, pp. 1-7, 2024. [CrossRef] [Google Scholar] [Publisher Link]

[31] Alejandro R. Ratazzi, Daniel H. Felix, and Gonzalo J. Gilardi, "Numerical Determination of Critical Local Buckling Loads in Thin and Open Wall Profiles Subjected to Flexural Compression Loads," *Structural Analysis*, vol. 41, no. 4, pp. 207-216, 2024. [CrossRef] [Google Scholar] [Publisher Link]

[32] J. Cervera et al., "Steel Compression Design: The Buckling's Weigth," *International Journal of Numerical Methods for Calculation and Design in Engineering*, vol. 29, no. 2, pp. 79-91, 2013. [CrossRef] [Google Scholar] [Publisher Link]

[33] BOE-A-2021-13681 Royal Decree, 2021. [Online]. Available: https://www.boe.es/buscar/doc.php?id=BOE-A-2021-13681

[34] Yichen Yang et al., "Global/Local Buckling Analysis of Thin-Walled I-Section Beams via Hierarchical One-Dimensional Finite Elements," *Engineering Structures*, vol. 280, 2023. [CrossRef] [Google Scholar] [Publisher Link]